Three dimensional scattering by an alluvial valley embedded in a fluid-saturated, poroelastic layered half-space for obliquely incident plane P1 waves

Z.N. Ba, & J.W. Liang
Department of Civil Engineering, Tianjin University, Tianjin

Z.N. Ba, & J.W. Liang
Key Laboratory of Coast Civil Structure Safety (Tianjin University), Ministry of Education, Tianjin

SUMMARY:
The indirect boundary element method (IBEM) is utilized to study three-dimensional responses of a two-dimensional alluvial valley in a fluid-saturated, poroelastic layered half-space for obliquely incident plane P1-waves in frequency domain, based on the three-dimensional exact dynamic stiffness matrix and moving Green's functions for the fluid-saturated, poroelastic layered half-space. The free-field responses are calculated to determine the displacements and stresses at the interface of the valley, and fictitious moving distributed loads and pore pressure are then applied at the interface to calculate the Green's functions for displacements and stresses. The amplitudes of the fictitious distributed loads and pore pressure are determined from the boundary conditions, and finally, the displacements arising from the waves in the free field and from the fictitious moving distributed loads and fictitious moving pore pressure are summed to obtain the solution.

Keywords: saturated-layered half space, three-dimensional scattering, alluvial valley, plane P1 waves

1. GENERAL INSTRUCTIONS

Local site in the form of valley can introduce large amplification of surface ground motion, and this phenomenon has been confirmed by field observations after large earthquakes. And in view of many buildings and structures are constructed atop of near valleys, the effect of valleys on seismic wave propagation has been the fundamental subject in seismology and earthquake engineering.

Diffraction of seismic waves by valleys may be solved analytically or numerically. Analytical methods are essential for exploring the physical nature of particular problem; however, numerical methods have the advantage in their applicability to problems with complex geometries and varying material properties, and in recent years, numerical methods developed rapidly with the development of high performance computers. Numerical methods such as the finite difference method (Boor *et al*, 1971), finite element method (Liao, 2002), boundary element method (Sesma *et al*, 1993), boundary integral equation method (Dravinski and Mossessian, 1987; Liang and Liu, 2009), discrete wave number method (Kawase and Aki, 1989), and modal superposition method (Semblat *et al*, 2005) have been applied to study the two dimensional seismic response of alluvial valley.

It should be noted that most of the contributions are still limited to the two dimensional waves scattering by a valley embedded in a uniform half space (either elastic half space or fluid-saturated, poroelastic half space), studies on the three-dimensional responses for a layered half space are relatively less. However, it has been reported that soil layers have an important effect on both the amplitudes and the spectrum of the ground motion (Liang and Ba, 2007; Ba and Liang, 2011). And it also has been reported that the three dimensional wave scattering is essentially different from the two dimensional case, the wave field cannot be simply decomposed into the valley axis direction and into the plane of the valley section and calculated as a superposition of the anti-plane results and the in-plane results (Liang et al, 2009; Liang et al, 2010; Barros and Luco, 1995).

In this paper, we present the indirect boundary element method (IBEM) to study the three dimensional wave scattering by an alluvial valley embedded in a fluid-saturated, poroelastic layered half-space for obliquely incident plane P1 waves. The IBEM yields very accurate results , with half space green's functions of moving distributed loads and of moving pore pressure acting on inclined lines in a fluid-saturated, poroelastic layered half-space as the fundamental solutions (Ba, 2008). The influence of key parameters, such as, angle of incidence, porosity, stiffness ratio of saturated soil layer to the underlying bedrock, and soil layer depth on the surface ground motion is studied and some useful conclusions are given.

2. CALCULATION MODEL AND METHOD

The geometry of the problem is shown in Fig. 1. A valley that is infinite in the direction of the y axis embedded in a fluid-saturated, poroelastic layered half-space composed by saturated soil layers and the underlying bedrock. The excitation is represented by plane P1 waves, which incident obliquely from the bedrock. The incoming wave arrives with an azimuth θ_h relative to the axis of the valley and an incidence θ_v to the vertical axis (see Fig.1). The profile of the valley cross section is shown in Fig. 1 (c).

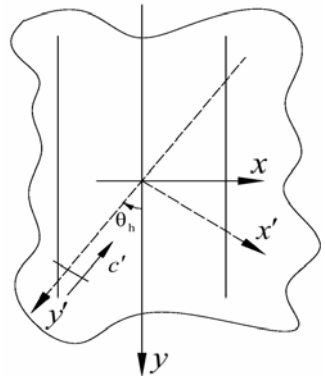

Figure 1. (a) Horizontal plane, definition of angle θ_h

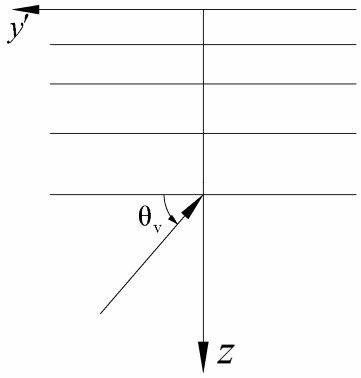

Figure 1. (b) Vertical plane, definition of angle θ_v

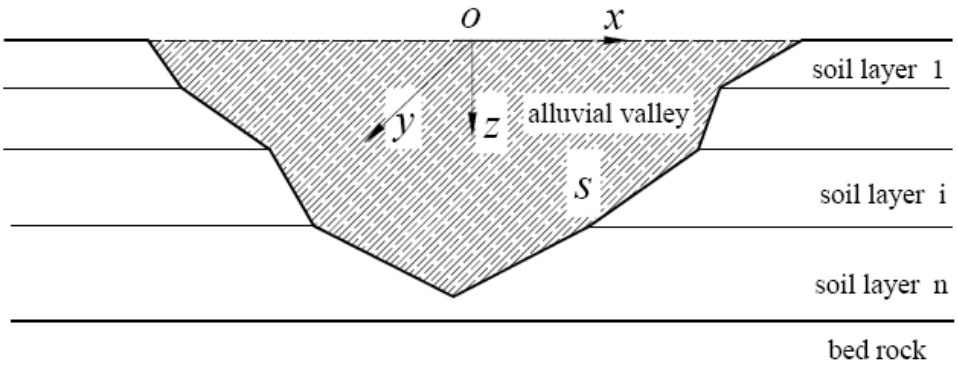

Figure 1. (c) Cross section of the valley

The total wave filed near the valley can be expressed as the superposition of the free field and the so called diffracted filed. The free field is the motion produced by the obliquely incident P1 waves in absence of the valley. At first, the free field response is calculated by the direct stiffness method. Then the diffracted fields in the valley and in the outside saturated layered half space are simulated by the dynamic responses produced by moving fictitious distributed loads and fictitious pore pressure imposed twice on the valley interface. And the densities of the moving distributed loads and pore pressure are obtained through the use of the continuity conditions along the valley interface. Finally,

the total motion is obtained by adding the free-filed motion and the diffracted-filed motion.

3. VERIFICATION

In case of a dry poroelastic solid (no fluid, $\rho_f = 0$), the presented solution should match that of the elastic half space studied by Barros and Luco (1995). Fig. 3 shows the surface displacements amplitudes around a semi-circular valley embedded in an elastic half space. Parameters are as follows: poisson's ratio $\mu = 1/3$, dimensionless incident frequency $\eta = \omega a / \pi c_s = 0.5$, damping ratio $\zeta = 0.005$, the shear wave velocity ratio of the valley to the half space is 0.5, the mass density ratio of the valley to the half space is 0.5 is 2/3, the vertical incident angle θ_v=30^0, 60^0 and 90^0, and the horizontal incident angle $\theta_h = 45^0$. Fig. 3 also shows that our results are satisfactory consistent with those of article Barros and Luco (1995).

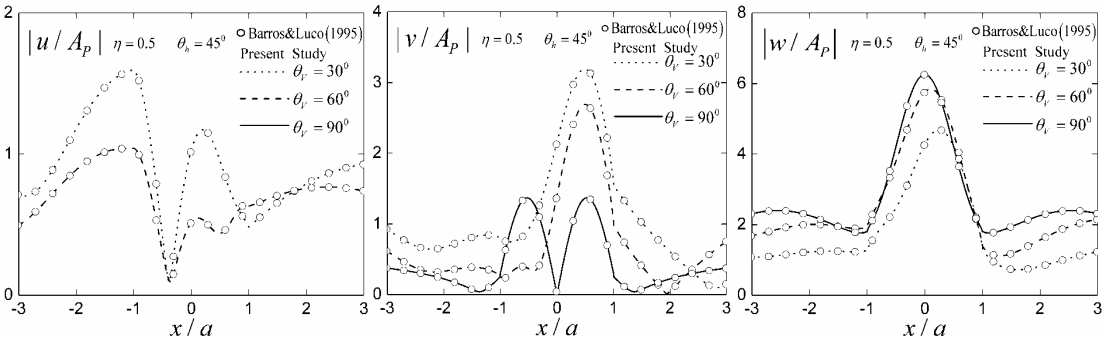

Figure 3. Comparison with results of Barros and Luco (1995)

4. NUMERICAL RESULTS

Fig. 4 presents the surface displacements amplitudes near a semi-circular valley embedded in a uniform saturated half space under undrained boundary condition for different obliquely incident angles. Parameters of the half space and of the valley are the same as in Liang and Liu (2009) shown in table 1, with superscript 'H' represents the half space and superscript 'V' represents the valley. We define the dimensionless incident frequency as $\eta = \omega a / \pi \sqrt{G^H / \rho^H}$, where ω is the incident circular frequency and a is the radius of the valley. Other parameters are as follows: η=0.5, θ_v=45^0, θ_h=0^0, 30^0, 60^0 and 90^0. $|U_x|$, $|U_y|$ and $|U_z|$ in Fig. 4 are again the solid frame displacements amplitudes and A_{P1} is the amplitude of incident plane P1 wave.

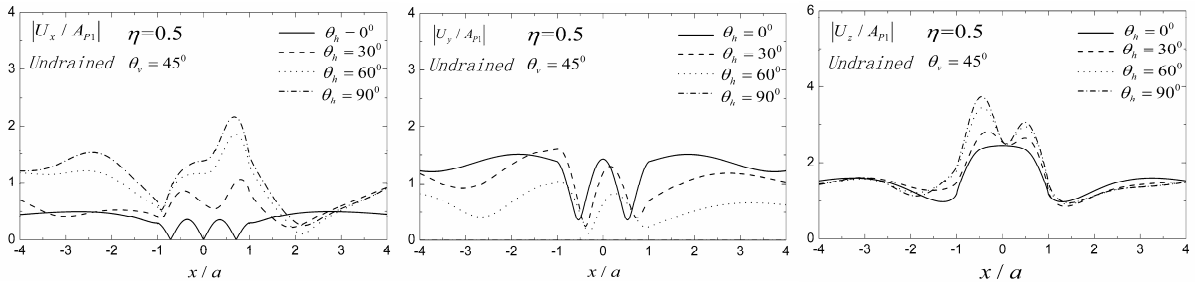

Fig. 4 Effects of obliquely incident angel on displacements amplitudes

Fig. 4 shows that the incident angle has a great effect on the displacements amplitudes. Generally, the horizontal displacements in the x direction increase gradually, while the displacements in the y direction decrease gradually, with the increasing horizontal angle of incidence (the angle between incident wave and the axis of the valley being larger). The reason for these phenomenon is that the vibration component along the x direction increase gradually with the incident direction tends to the x axis.

Table 1 Parameters for the saturated half space and valley used in Liang and Liu (2009)

n^H	G^H	ρ_s^H	ρ_f^H	M^H	m^H	υ^H	α^H	ζ^H
0.3	37E8	2650	1000	60.72E8	7222	0.25	0.8287	0.05
n^V	G^V	ρ_s^V	ρ_f^V	M^V	m^V	υ^V	α^V	ζ^V
0.3	9.25E8	2650	1000	47.92E8	7222	0.25	0.8287	0.05

Fig. 5 illustrates the surface displacement amplitudes around a valley embedded in a uniform saturated poroelastic half space under undrained boundary condition for different porosities $n=0.1$, 0.3 and 0.34. The material parameters used are given in table 1. And the other parameters for calculation are as follows: horizontal incident angle θ_h=45^0, vertical incident angle θ_v=5^0, 30^0 and 60^0, and the dimensionless incident frequency η=1.0.

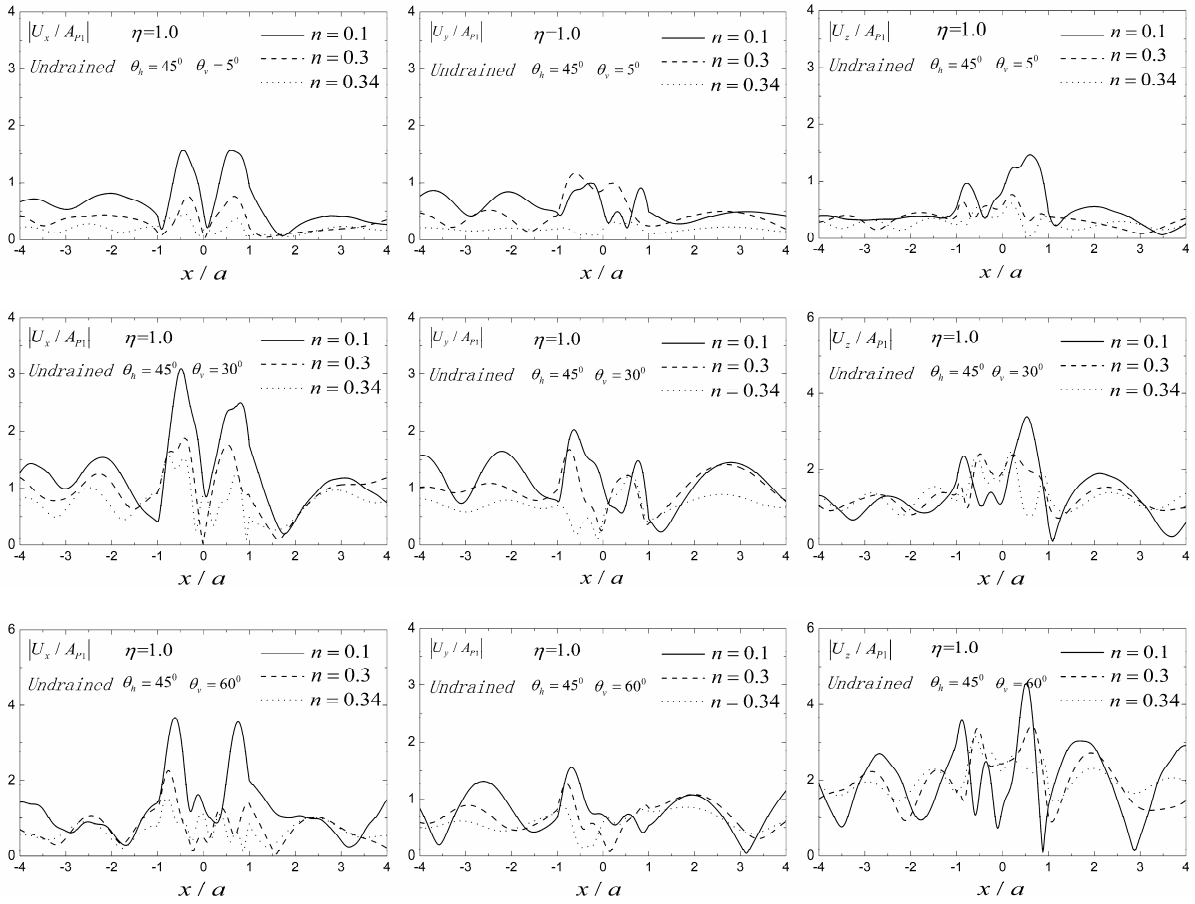

Fig. 5 Displacements amplitudes for different porosity

Fig. 5 shows that porosity has significant effect on wave scattering around the valley embedded in a saturated poroelastic half space. Large difference for displacement amplitudes and large phase shifts can be observed. The amplitudes of the horizontal displacements decrease gradually with the increasing of the porosity, which may be due to the smaller horizontal displacement amplitudes of the free-field for larger porosity. It can also be seen form Fig. 5 that the displacement amplitudes in the x- and z- directions are more complex compared with the amplitudes in the y- direction. The differences may be due to the infinity of the valley in the y- direction.

To study the wave scattering and diffraction by valley embedded in a layered saturated poroelastic half space, Fig. 6 presents displacement amplitudes around a semi-circular valley embedded in a single saturated poroelastic soil layer overlying bedrock for obliquely incident planer P1 waves under drained boundary. The material parameters used are given in table 2 with superscript 'L' represents the saturated layer and superscript 'V' represents the valley. The parameters of the elastic bedrock are as follows: mass density $\rho^R = 1855 KN/m^3$, poisson's ratio v^R=0.25, damping ratio ζ^R=0.02, and the shear module ratio of the bedrock to the layer is $\sqrt{G^R/G^L} = 2.0$ and $\sqrt{G^R/G^L} = 5.0$. The thickness of the soil layer is $H/a = 2.0$ .The dimensionless frequency is defined as $\eta = \omega a/\pi\sqrt{G^L/\rho^L}$ and $\eta = 0.5$ and 0.75 is chosen in Fig. 6. The horizontal incident angle is θ_h=45^0, the vertical incident angles are θ_v=5^0, 30^0, 60^0 and 90^0. The dimensionless displacement amplitudes in Fig. 6 is the ratio of between the displacement amplitudes of the surface displacement with the amplitude of the incident P1 waves A_{P1}.

Table 2 parameters for the saturated soil layer and the valley

n^L	G^L	ρ_s^L	ρ_f^L	M^L	m^L	v^L	α^L	ζ^L
0.3	37E8	2650	1000	60.72E8	7222	0.25	0.8287	0.05
n^V	G^V	ρ_s^V	ρ_f^V	M^V	m^V	υ^V	α^V	ζ^V
0.3	9.25E8	2650	1000	47.92E8	7222	0.25	0.8287	0.05

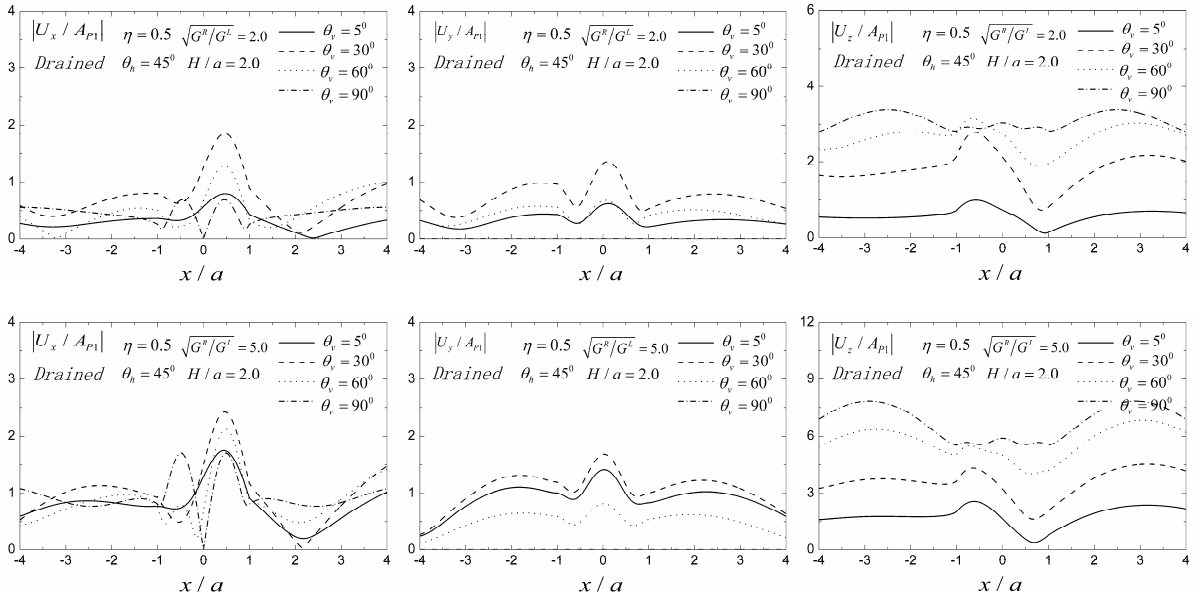

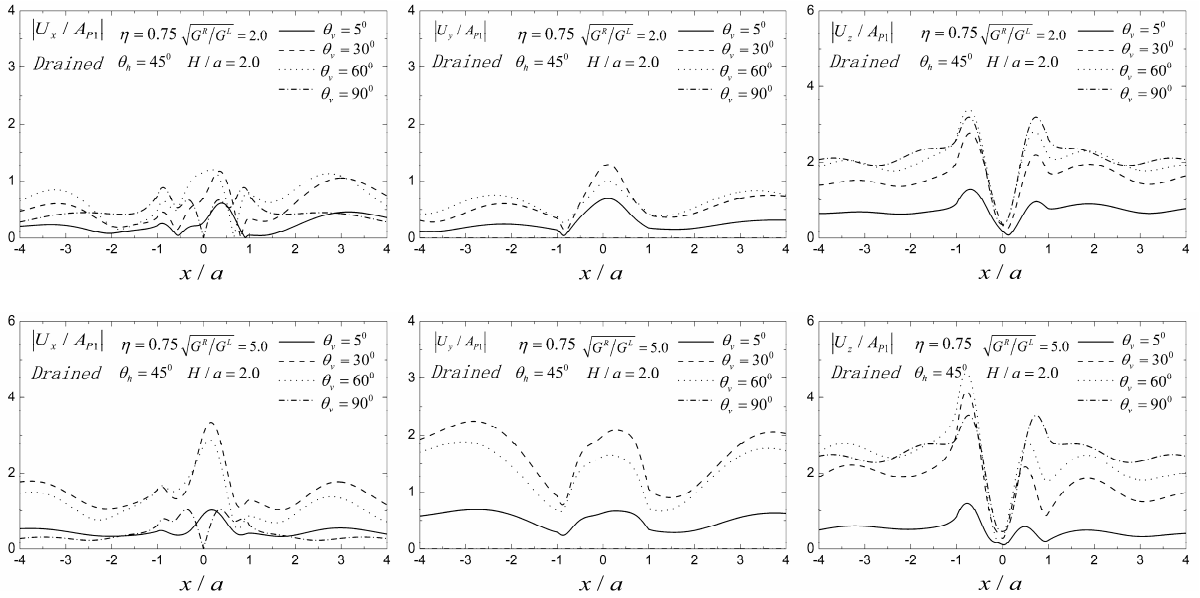

Fig. 6 Displacements amplitudes for different dynamic stiffness ratio between bedrock to saturated layer

It is shown that the surface displacement amplitudes can differ greatly between the layered half space and the uniform half space, depending on the dimensionless frequencies and obliquely incident angles. It is because that the displacements for the layered half space are determined by the dynamic characters of the valley and also the soil layer for a given dimensionless frequency and obliquely incident angle, while the displacements for the uniform half space can only be determined by the dynamic characters of the valley. It can be seen from Fig. 6 that, when the frequency of the incident waves near a resonant frequency of the layer (η=0. 5), the displacement amplitudes for the layered half space are significantly larger than that for the uniform half space. The results in Fig. 6 show that the differences between the uniform and layered cases cannot be solely attributed to the differences in the free-field ground motion, and there is some interaction between the valley and the soil layer. It can also be concluded that, although the ratio between the bedrock to the saturated soil layer changed, the distribution of the surface displacement amplitudes just looks similar. To explain this, it may be convenient to think the unchanged self dynamic characteristic as the thickness of the soil layer keeps invariant.

To study the influence of soil layer depth, Fig.7 present the surface displacement amplitudes around a semi-circular valley embedded in a single saturated poroelastic soil layer overlying bedrock for obliquely incident planer P1 waves under drained boundary for different soil layer thickness H/a=1.0 and H/a=4.0. The same model is used as in Fig. 6. The ratio of the bedrock to the saturated soil layer $\sqrt{G^R/G^L}$=5.0 and dimensionless incident frequency η=0.5 are adopted with the other parameters are the same with those in Fig. 6.

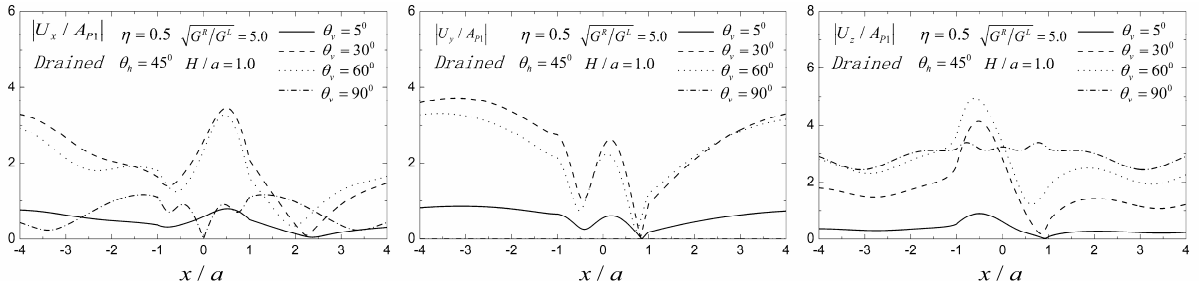

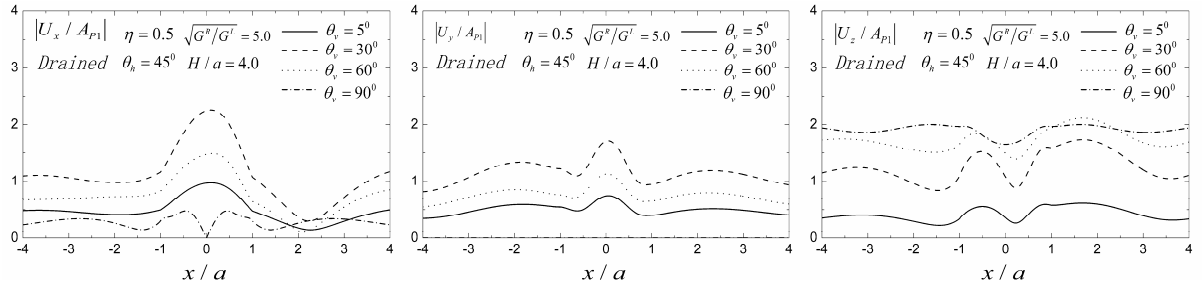

Fig. 7 Displacements amplitudes for different soil layer depth

Comparison the results in Fig. 7 with those of in Fig. 6, we find that the soil layer depth has significant effect not only on the amplitudes but also the distribution of the surface displacements. For the given dimensionless incident frequency η=0.5, the surface displacement amplitudes distribution is entirely different corresponding to different soil layer depth H/a=1.0, 2.0 and 4.0, and this may be due to the change of the soil layer depth directly changed the self dynamic characteristic of the layered site. It can also be seen that the displacement amplitudes decrease gradually as the soil layer increasing, and this is because the material damping of the valley and the soil layer are considered and the control point is selected at the outcrop of the bedrock.

4. **CONCLUSIONS**

The three dimensional scattering of obliquely incident plane P1 waves by an alluvial valley embedded in a saturated poroelastic layered half space is studied by the indirect boundary element method in the frequency domain. The direct stiffness method is used to calculate the free field responses, and green's functions of moving distributed loads and pore pressure acting on inclined lines are used to simulate the diffraction wave field in the layered half space and in the valley. Numerical results and analyses are performed by taking the valley embedded in a uniform saturated poroelastic half space and in a single saturated poroelastic soil layer overlying on elastic bedrock as examples, and the following conclusions are obtained.

(1) The angel of incidence has significant effect on the surface displacement amplitudes. Generally, the surface displacement amplitudes in the $x-$ direction increase gradually with the increasing horizontal incident angle (the incident direction gradually tends to the x axis).

(2) The porosity has important effect on the surface displacement amplitudes. Large differences for displacement amplitudes and large phase shifts are observed depending on different porosities.

(3) The surface displacement amplitudes can differ greatly between the layered half space and the uniform half space. The dynamic responses for the layered half space are determined by the interaction of the soil layers with the valley. The ratio between the bedrock to the saturated poroelastic soil layer affects the amplitudes of the surface displacement, while the depth of the soil layer affects not only the amplitudes but also the spatial distribution of the surface displacements.

AKCNOWLEDGEMENT
This study is supported by the National Natural Science Foundation (NO. 50908156 and NO. 50978183) and Tianjin Natural Science Foundation (12JCQNJC04700)

REFERENCES

Boore, D.M., Larner, K.L. and Aki, K. (1971). Comparison of two independent methods for the solution of wave scattering problems: response of a sedimentary basin to incident SH waves. *J Geophysical Research* **76**,558-569

Liao, Z.P. (2002), Introduction to wave motion theories in engineering, Science Press

Sainchez-Sesma, F.J., Ramos-Martinez, J. and Campillo M. (1993). An indirect boundary element method applied to simulate the seismic response of alluvial valleys for incident P, S and Rayleigh Waves. *Earthquake Eng Struct Dyn* **22**, 279-295

Dravinski, M. and Mossessian, T.K. (1987). Scattering of plane harmonic P, SV, and Rayleigh waves by dipping layers of arbitrary shape. *Bull Seism Soc Am* **77**, 212-235

Liang, J.W. and Liu, Z.X. (2009). Diffraction of plane P waves by a canyon of arbitrary shape in poroelastic half-space (I): Formulation. *Earthquake Science* **22:3**,215-222

Liang, J.W. and Liu, Z.X. (2009). Diffraction of plane P waves by a canyon of arbitrary shape in poroelastic half-space (II): Numerical results and discussions. *Earthquake Science* **22:3**,223-230

Kawase, H. and Aki, K. (1989). A Study on the response of a soft basin for incident S, P and Rayleigh waves with special reference to the long duration observed in Mexico city. *Bull Seism Soc Am* **79:5**,1361-1382,

Semblat, J.F., Kham M., Parara E., et.al. (2005). Seismic wave amplification: Basin geometry vs soil layering. *Soil Dyn Earthq Eng* **25**, 529-538

Liang, J.W. and Ba, Z.N. (2007). Surface motion of an alluvial valley in layered half-space for incident plane SH waves. *Journal of Earthquake Engineering and Engineering Vibration* **27:3**: 1-9

Ba, Z.N. and Liang, J.W. (2011). Surface Motion of an Alluvial Valley in Layered Half-Space for Incident Plane P-Waves. *Transactions of Tianjin University* **17:3**,157-165

Ba, Z.N. and Liang, J.W. (2011). Diffraction of plane SV waves around an alluvial valley in layered half-space. *Journal of Earthquake Engineering and Engineering Vibration* **31:3**,18-26

Liang, J.W., Wei, X.L. and Lee, V.W. (2009). 3D scattering of plane SV waves by a circular-arc alluvial valley. *Chinese Journal of Geotechnical Engineering* **31:9**,1345-1353

Liang, J.W., Wei, X.L. and Lee, V.W. (2010). 3D scattering of plane P waves by a circular-arc alluvial valley. *Rock and Soil Mechanics* **31:1**,461-470

Liang, J.W., Wei, X.L. and Lee, V.W. (2009). Analytical Solution for 3D Scattering of Rayleigh Waves by a Circular-Arc Alluvial Valley. *Journal of Tianjin University* **42:1**,24-34

De Barros, F.C.P. and Luco, J.E. (1995). Amplication of obliquely incident waves by a cylindrical valley embedded in a layered half-space. *Soil Dyn Earthq Engng* **14**,163-175

Ba, Z.N. (2008), Green's Functions for Layered Half Space and Elastic Wave Scattering by Local Sites. *PHD thesis*, Tianjin University, Tianjin

Biot, M.A. (1956). The theory of propagation of elastic waves in a fluid-saturated porous solid I: Low-frequency range *J Acoust Soc Am* **28**,168-178

Biot, M.A. (1956). The theory of propagation of elastic waves in a fluid-saturated porous solid II: Higher-frequency range. *J Acoust Soc Am* **28**,179-191

Lin, C.H., Lee, V.W. and Trifunac, M.D. (2005). The reflection of plane waves in a poroelastic half-space fluid saturated with inviscid fluid. *Soil Dyn Earthquake Eng* **25**,205-223